

# Organometallic Nickel(III) Complexes Relevant to Cross-Coupling and Carbon–Heteroatom Bond Formation Reactions

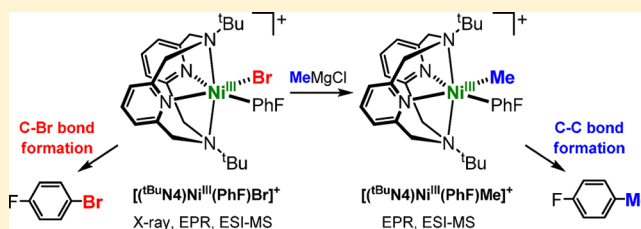
Bo Zheng,<sup>†</sup> Fengzhi Tang,<sup>†</sup> Jia Luo,<sup>†</sup> Jason W. Schultz,<sup>†</sup> Nigam P. Rath,<sup>‡</sup> and Liviu M. Mirica<sup>\*,†</sup>

<sup>†</sup>Department of Chemistry, Washington University, One Brookings Drive, St. Louis, Missouri 63130-4899, United States

<sup>‡</sup>Department of Chemistry and Biochemistry, University of Missouri-St. Louis, One University Boulevard, St. Louis, Missouri 63121-4400, United States

**S** Supporting Information

**ABSTRACT:** Nickel complexes have been widely employed as catalysts in C–C and C–heteroatom bond formation reactions. In addition to Ni(0) and Ni(II) intermediates, several Ni-catalyzed reactions are proposed to also involve odd-electron Ni(I) and Ni(III) oxidation states. We report herein the isolation, structural and spectroscopic characterization, and organometallic reactivity of Ni(III) complexes containing aryl and alkyl ligands. These Ni(III) species undergo transmetalation and/or reductive elimination reactions to form new C–C or C–heteroatom bonds and are also competent catalysts for Kumada and Negishi cross-coupling reactions. Overall, these results provide strong evidence for the direct involvement of organometallic Ni(III) species in cross-coupling reactions and oxidatively induced C–heteroatom bond formation reactions.



## INTRODUCTION

Nickel complexes have been employed in catalytic organometallic transformations such as Negishi, Kumada, and Suzuki cross-coupling reactions.<sup>1–6</sup> By contrast to the thorough mechanistic understanding of the widely used Pd-catalyzed cross-coupling reactions, the mechanisms of Ni-catalyzed reactions are not fully understood, as Ni can undergo more easily both one- and two-electron redox reactions, and the presence of paramagnetic species makes reactivity studies more difficult. While the involvement of Ni<sup>III</sup> (and Ni<sup>I</sup>) oxidation states in cross-coupling reactions<sup>7–31</sup> and oxidatively induced C–heteroatom bond formation reactions<sup>32–36</sup> is more commonly accepted than for Pd, to the best of our knowledge no organometallic Ni<sup>III</sup> species that can undergo C–C or C–heteroatom bond formation reactions have been isolated or characterized to date.

Organometallic Ni<sup>III</sup> species have also been proposed as catalytically active intermediates in metalloenzymes such as methyl-coenzyme M reductase (MCR)<sup>37,38</sup> and carbon monoxide dehydrogenase/acetyl-CoA-synthetase (CODH/ACS).<sup>39,40</sup> For example, a Ni<sup>III</sup>-methyl species has been characterized by EPR in MCR,<sup>41,42</sup> and also structurally characterized in two synthetic systems.<sup>43,44</sup> Interestingly, organometallic Ni<sup>III</sup> intermediates have also been recently proposed to play a role in the C–H activation step during the anaerobic oxidation of methane by methanotrophic archaea.<sup>45,46</sup>

Herein we report the isolation and characterization of a series of Ni<sup>III</sup>(aryl)halide complexes stabilized by the tetradentate ligand *N,N'*-di-*tert*-butyl-2,11-diaza[3.3](2,6)pyridinophane (<sup>t</sup>BuN4), which was recently employed by us to stabilize

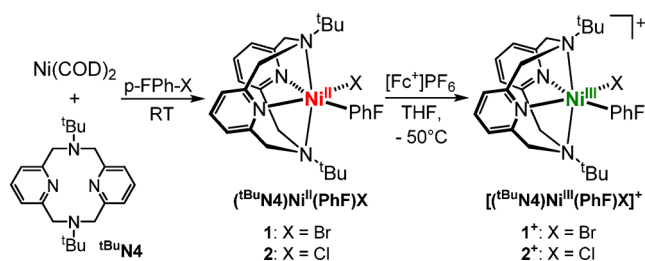
uncommon mononuclear Pd<sup>III</sup> complexes.<sup>47–50</sup> The described organometallic Ni<sup>III</sup> species exhibit structural and electronic properties that suggest a metal-based radical description, in line with the presence of a Ni<sup>III</sup> center. These complexes are stable at low temperature, yet they undergo rapid C–halide bond formation at room temperature, providing evidence that such Ni<sup>III</sup> species are the active intermediates in oxidatively induced C–heteroatom bond formation reactions. The characterized Ni<sup>III</sup>(aryl)halide complexes undergo rapid transmetalation with Grignard or organozinc reagents to yield detectable Ni<sup>III</sup>(aryl)-alkyl species followed by C–C bond formation, strongly supporting their role as intermediates in Kumada and Negishi cross-coupling reactions. In addition, one-electron oxidation of an isolated Ni<sup>II</sup>(aryl)alkyl complex leads to rapid formation of reductive elimination products, and both (<sup>t</sup>BuN4)Ni<sup>II</sup> and (<sup>t</sup>BuN4)Ni<sup>III</sup> species are active catalysts for Kumada and Negishi cross-coupling reactions. Overall, these studies provide for the first time strong evidence for the direct involvement of organometallic Ni<sup>III</sup> complexes in Ni-mediated cross-coupling reactions and oxidatively induced C–heteroatom bond formation reactions.

## RESULTS AND DISCUSSION

**Synthesis and Characterization of  $[(t\text{BuN}4)\text{Ni}^{\text{III}}\text{ArX}]^+$  Complexes.** The Ni<sup>II</sup> precursors (<sup>t</sup>BuN4)Ni<sup>II</sup>(PhF)X (PhF = *p*-fluorophenyl; X = Br: 1; X = Cl: 2) were prepared by the oxidative addition of the corresponding aryl halides to Ni(COD)<sub>2</sub> in the presence of <sup>t</sup>BuN4 (Scheme 1).<sup>51</sup> In these

Received: March 11, 2014

Published: April 8, 2014

**Scheme 1. Synthesis of  $({}^t\text{BuN4})\text{Ni}^{\text{II}}$  and  $({}^t\text{BuN4})\text{Ni}^{\text{III}}$  complexes**


complexes,  ${}^t\text{BuN4}$  acts as a tetradentate ligand, and the aryl and halide group complete the distorted octahedral coordination geometry of the  $\text{Ni}^{\text{II}}$  center, similar to other reported  $({}^t\text{BuN4})\text{Ni}^{\text{II}}\text{X}_2$  complexes.<sup>52,53</sup> The deviation from the octahedral geometry likely results from the small ring size of the  ${}^t\text{BuN4}$  macrocyclic ligand and the bulky *t*-butyl N-substituents.<sup>47,48,50</sup> This geometry is confirmed by single crystal X-ray diffraction analysis of **1** that reveals an average axial Ni– $\text{N}_{\text{amine}}$  bond length of 2.385 Å that is longer than the average equatorial Ni– $\text{N}_{\text{pyridyl}}$  bond length of 2.036 Å (Figure 1A). Complexes **1** and **2**

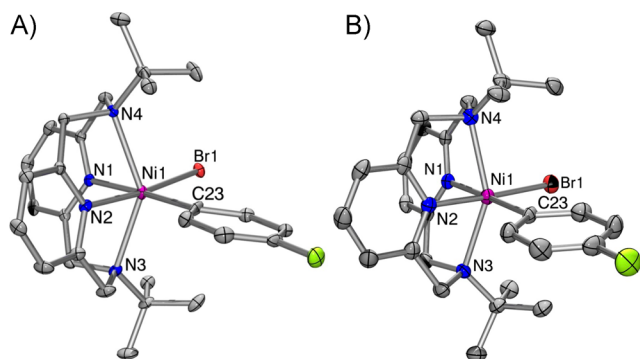


**Figure 1.** ORTEP representation of **1** (A) and the cation of  $[\mathbf{1}^+]\text{PF}_6$  (B) with 50% probability thermal ellipsoids. Selected bond lengths (Å): **1**: Ni1–N1 2.046; Ni1–N2 2.025; Ni1–N3 2.364; Ni1–N4 2.406; Ni1–C23 2.061; Ni1–Br1 2.643; **1**<sup>+</sup>: Ni1–N1 1.965; Ni1–N2 1.928; Ni1–N3 2.323; Ni1–N4 2.305; Ni1–C23 2.018; Ni1–Br1 2.395.

are paramagnetic, suggesting an  $S = 1$  ground state as expected for octahedral high-spin  $\text{Ni}^{\text{II}}$  centers; this is confirmed by the effective magnetic moment  $\mu_{\text{eff}}$  of 2.89  $\mu_{\text{B}}$  for **1** determined by the Evans method.<sup>54</sup> Interestingly, cyclic voltammetry scans of **1** and **2** in MeCN reveal reversible oxidation waves at –450 and –400 mV vs  $\text{Fc}^+/\text{Fc}$ , respectively. These oxidative processes are tentatively assigned to the  $\text{Ni}^{\text{II}}/\text{Ni}^{\text{III}}$  couple and suggest that the  $\text{Ni}^{\text{III}}$  oxidation state should be accessible for this ligand system.

Due to their low oxidation potentials, complexes **1** and **2** can be readily oxidized with 1 equiv  $[\text{Fc}^+]\text{PF}_6$  in THF at –50 °C to yield the temperature-sensitive green products  $[({}^t\text{BuN4})\text{Ni}^{\text{III}}(\text{PhF})\text{Br}]^+$ , **1**<sup>+</sup>, and  $[({}^t\text{BuN4})\text{Ni}^{\text{III}}(\text{PhF})\text{Cl}]^+$ , **2**<sup>+</sup>, respectively. Characterization by X-ray diffraction of crystals of  $[\mathbf{1}^+]\text{PF}_6$  and  $[\mathbf{2}^+]\text{PF}_6$  (obtained from THF/pentane solutions) confirms the identity of these species and shows the metal centers adopt a distorted octahedral geometry (Figures 1B and S46), with axial Ni– $\text{N}_{\text{amine}}$  bond lengths (2.305–2.323 Å) that are greater than the axial Ni– $\text{N}_{\text{pyridyl}}$  bond lengths (1.903–1.965 Å) and similar to the only two other six-coordinate organometallic  $\text{Ni}^{\text{III}}$  complexes reported by van Koten et al.<sup>55,56</sup>

The observed distorted octahedral geometries of the  $\text{Ni}^{\text{III}}$  centers are also in line with the Jahn–Teller-like distortions expected for  $d^7$  ions. In both **1**<sup>+</sup> and **2**<sup>+</sup>, the Ni– $\text{N}_{\text{pyridyl}}$  bond that is *trans* to the aryl group is longer than the Ni– $\text{N}_{\text{pyridyl}}$  bond *trans* to the halide, due to the stronger *trans* influence of the C-donor ligand. The Ni– $\text{C}_{\text{aryl}}$  distance in **1**<sup>+</sup> (2.02 Å) is slightly longer than those in the few other reported  $\text{Ni}^{\text{III}}$ –aryl complexes.<sup>55–58</sup>

Complexes  $[\mathbf{1}^+]\text{PF}_6$  and  $[\mathbf{2}^+]\text{PF}_6$  are paramagnetic and exhibit effective magnetic moments  $\mu_{\text{eff}}$  of 2.11–2.03  $\mu_{\text{B}}$  at –20 °C, corresponding to one unpaired electron.<sup>54</sup> The EPR spectra (77 K, 1:1 THF:PrCN glass) reveal rhombic signals and  $g_{\text{ave}} = 2.160$ –2.162, along with superhyperfine coupling to the two axial N donors ( $I = 1$ ) observed in the  $g_z$  direction (Figure 2A).

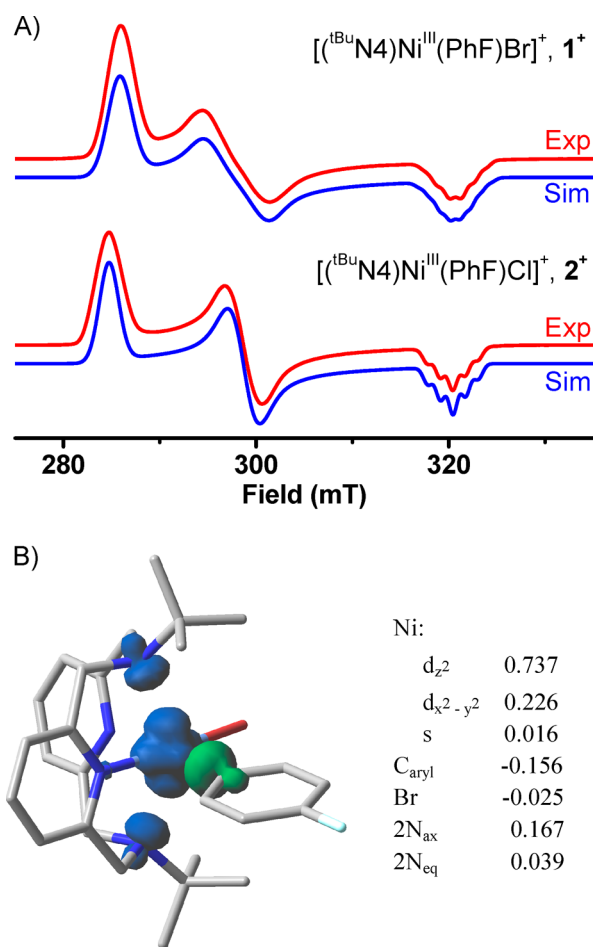


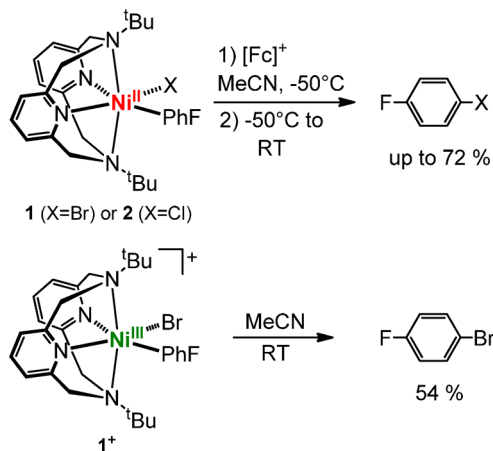
**Figure 2.** (A) EPR spectra (red lines) of **1**<sup>+</sup> (top) and **2**<sup>+</sup> (bottom) in 1:1 THF:PrCN at 77 K, and the simulated EPR spectra (blue lines) using the following parameters: **1**<sup>+</sup>,  $g_x = 2.272$ ;  $g_y = 2.180$  ( $A_{\text{Br}} = 16.0$  G);  $g_z = 2.026$  ( $A_{\text{N}}(2\text{N}) = 12.0$  G,  $A_{\text{Br}} = 11.7$  G); **2**<sup>+</sup>,  $g_x = 2.282$ ;  $g_y = 2.175$ ;  $g_z = 2.028$  ( $A_{\text{N}}(2\text{N}) = 13.0$  G). (B) DFT calculated Mulliken spin density for **1**<sup>+</sup> (shown as a 0.005 isodensity contour plot), and the relevant atomic and Ni orbital contributions to the spin density.

In addition, superhyperfine coupling to the Br atom ( $I = 3/2$ ) is observed for **1**<sup>+</sup> along the  $g_y$  and  $g_z$  directions. Taken together, the observed structural and EPR parameters for  $[\mathbf{1}^+]\text{PF}_6$  and  $[\mathbf{2}^+]\text{PF}_6$  strongly suggest the presence of a distorted octahedral  $d^7$   $\text{Ni}^{\text{III}}$  center in a  $d_{z^2}$  ground state.<sup>55–59</sup> Density functional theory (DFT) calculations support a metal-based radical description for these complexes, and the calculated spin density for **1**<sup>+</sup> shows the unpaired electron resides mostly (>98%) on

the Ni center, with a major (74%) and minor (22%) contribution from the  $3d_{z^2}$  and  $3d_{x^2-y^2}$  Ni orbitals, respectively (Figure 2B). The appreciable contribution from the  $3d_{x^2-y^2}$  orbital also supports the observed superhyperfine coupling to the equatorial Br ligand, while the calculated  $g$  values and coupling constants for  $1^+$  and  $2^+$  are similar to the experimental values (Table S16). In addition, the time-dependent DFT (TD-DFT) calculated UV-vis spectra reproduce well the two electronic absorptions observed for both  $1^+$  and  $2^+$  at  $\sim 650$  and  $\sim 1000$  nm (Figures S41 and S42), which are assigned to ligand-to-metal charge transfer transitions (Tables S13 and S14).

**C-Halide Bond Formation Reactivity of  $[(t^{\text{Bu}}\text{N}4)\text{Ni}^{\text{III}}\text{ArX}]^+$  Complexes.** The isolation of the organometallic  $\text{Ni}^{\text{III}}$  complexes  $[1^+]\text{PF}_6$  and  $[2^+]\text{PF}_6$  allowed the direct investigation of their reactivity, as such  $\text{Ni}^{\text{III}}$  species have been proposed as intermediates in oxidatively induced C–O,<sup>32,34,35</sup> C–N,<sup>33,36</sup> C–halide,<sup>60–62</sup> and C–S<sup>63</sup> bond formation reactions from  $\text{Ni}^{\text{II}}$  precursors as well as H atom abstraction reactions.<sup>59</sup> Oxidation of **1** or **2** by  $[\text{Fc}^+]\text{PF}_6$  in MeCN generates the corresponding EPR-detectable  $\text{Ni}^{\text{III}}$  species, which then undergo C–halide bond formation to generate *p*-fluorophenyl bromide (*p*-FPh-Br) or *p*-fluorophenyl chloride (*p*-FPh-Cl) in up to 72% yield (Scheme 2). The reductive

**Scheme 2. C–halide Bond Formation Reactivity of Organometallic  $(t^{\text{Bu}}\text{N}4)\text{Ni}^{\text{II}}$  and  $(t^{\text{Bu}}\text{N}4)\text{Ni}^{\text{III}}$  Complexes**

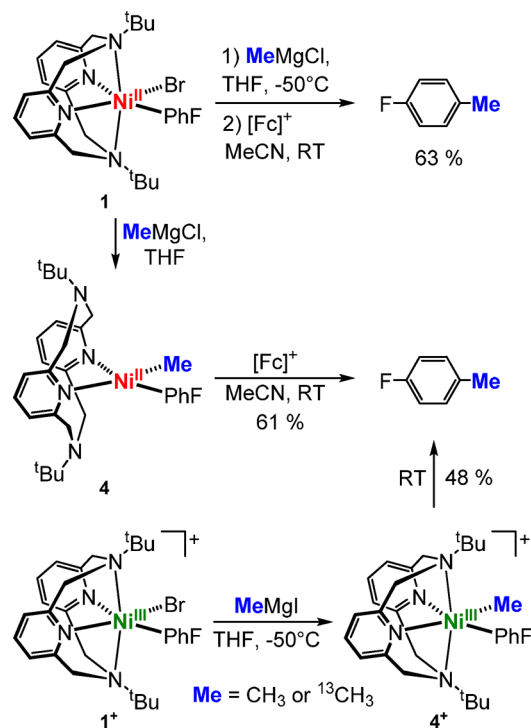


elimination from the  $1^+$  or  $2^+$  species is proposed to yield an unstable  $\text{Ni}^{\text{I}}$  species that undergoes rapid disproportionation to  $\text{Ni}^0$  and a  $[(t^{\text{Bu}}\text{N}4)\text{Ni}^{\text{II}}(\text{halide})(\text{MeCN})]^+$  species, as observed experimentally.<sup>54</sup> Complex  $2^+$  is less stable than  $1^+$  in solution as it likely undergoes ligand exchange and reduction more easily; thus, most reactivity experiments were performed using isolated or *in situ* generated  $1^+$ . When an MeCN solution of  $[1^+]\text{PF}_6$  is warmed up to RT, *p*-FPh-Br is formed in 54% yield (Scheme 2). In order to probe the mechanism of reductive elimination, a 1:1 mixture of **1** and  $(t^{\text{Bu}}\text{N}4)\text{Ni}^{\text{II}}(\text{PhMe})\text{Cl}$ , **3**, in MeCN was treated with  $[\text{Fc}^+]\text{PF}_6$  (1 equiv per Ni), and analysis of the reaction mixture reveals the formation of *p*-FPh-Br and *p*-MePh-Cl as well as *p*-FPh-Cl and *p*-MePh-Br.<sup>54</sup> Moreover, similar yields of the C–halide bond formation products were observed when a 1:1 mixture in THF of  $[1^+]\text{PF}_6$  and  $[(t^{\text{Bu}}\text{N}4)\text{Ni}^{\text{III}}(\text{PhMe})\text{Cl}]\text{PF}_6$ ,  $[3^+]\text{PF}_6$ , was warmed up to RT, while no ligand exchange was observed at the  $\text{Ni}^{\text{III}}$  center when the mixture was kept at  $-50$  °C for 8 h. The formation of the crossover products suggests an initial halide dissociation step followed by C–halide bond formation, similar to what was

previously proposed by Hillhouse et al. for C–N bond formation at a  $\text{Ni}^{\text{III}}$  center.<sup>36</sup> Overall, these experiments provide strong evidence for the ability of  $\text{Ni}^{\text{III}}$ (aryl)halide species to act as the key intermediates in oxidatively induced C–heteroatom bond formation from  $\text{Ni}^{\text{II}}$  precursors.<sup>32–36,60</sup>

**C–C Bond Formation Reactivity of Organometallic  $(t^{\text{Bu}}\text{N}4)\text{Ni}^{\text{III}}$  Complexes.** In addition to C–heteroatom bond formation reactions, organometallic  $\text{Ni}^{\text{III}}$  species have been proposed as catalytically active intermediates in Kumada and Negishi cross-coupling reactions.<sup>7–31</sup> In these transformations a key  $\text{Ni}^{\text{III}}$ -dihydrocarbyl species, formed either upon one-electron oxidation of a  $\text{Ni}^{\text{II}}$ -dihydrocarbyl precursor or transmetalation of a  $\text{Ni}^{\text{III}}$ -monohydrocarbyl species, is assumed to undergo reductive elimination to generate the cross-coupled product. However, while the formation of a transient bis(trifluoromethyl) $\text{Ni}^{\text{III}}$  species has been reported recently by Vici et al.,<sup>64</sup> no  $\text{Ni}^{\text{III}}$ -dihydrocarbyl species has been isolated to date and observed to undergo C–C bond formation. In order to probe the reactivity of such organometallic Ni species, the complex  $(t^{\text{Bu}}\text{N}4)\text{Ni}^{\text{II}}(\text{PhF})\text{Me}$ , **4**, was synthesized by transmetalation of **1** with 1 equiv MeMgCl in THF (Scheme 3). The

**Scheme 3. C–C Bond Formation Reactivity of Organometallic  $(t^{\text{Bu}}\text{N}4)\text{Ni}^{\text{II}}$  and  $(t^{\text{Bu}}\text{N}4)\text{Ni}^{\text{III}}$  Complexes**



single crystal X-ray analysis of **4** reveals a square planar geometry for the  $\text{Ni}^{\text{II}}$  center with the two pyridyl N atoms and the two organic ligands bonded to Ni (Figure 3), in contrast to the distorted octahedral geometry of complexes **1** and **2**. The lack of axial interactions in **4** is likely due to the presence of two strong  $\sigma$ -donor organic ligands. In addition, **4** is diamagnetic, as expected for a square planar low-spin  $\text{Ni}^{\text{II}}$   $d^8$  center and in contrast to the high-spin paramagnetic complexes **1** and **2**.

Gratifyingly, when **4** is oxidized by  $[\text{Fc}^+]\text{PF}_6$  in MeCN, the C–C bond formation product, *p*-FPh-Me, is generated in 61% yield (Scheme 3). A small amount of fluorobenzene (PhF) is also produced during the oxidatively induced C–C bond

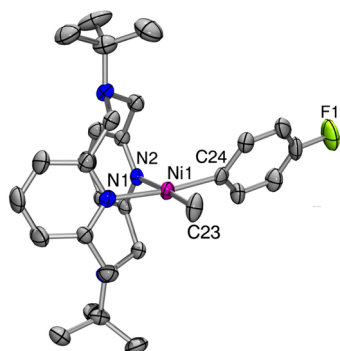


**Figure 3.** ORTEP representation of **4** with 50% probability thermal ellipsoids. Selected bond lengths (Å): Ni1–N1 1.987; Ni1–N2 1.975; Ni1–C23 1.921; Ni1–C24 1.902.

formation reactivity of **1**, and PhF most likely forms by the reaction of **3**<sup>+</sup> with the trace amount of water present in the solvent.<sup>54</sup> ESI-MS analysis of the oxidation of **1** performed at –50 °C reveals an *m/z* peak at 520.2524 that was assigned to [(<sup>t</sup>BuN4)Ni<sup>III</sup>(PhF)Me]<sup>+</sup>, **4**<sup>+</sup> (calculated *m/z*: 520.2507, Figure S11), while oxidation of (<sup>t</sup>BuN4)Ni<sup>II</sup>(PhF)(<sup>13</sup>CH<sub>3</sub>), **13C-4**, with 1 equiv [Fc<sup>+</sup>]PF<sub>6</sub> generates a species with an *m/z* peak at 521.2544 corresponding to [(<sup>t</sup>BuN4)Ni<sup>III</sup>(PhF)(<sup>13</sup>CH<sub>3</sub>)]<sup>+</sup> (calculated *m/z*: 521.2545, Figure S11). A similar yield of *p*-FPh-Me (63%) is obtained from the *in situ* transmetalation of **1** with 1 equiv MeMgCl followed by oxidation with 1 equiv [Fc<sup>+</sup>]PF<sub>6</sub> (Scheme 3). The intermediacy of the Ni<sup>III</sup>(aryl)alkyl species **4**<sup>+</sup> during C–C bond formation is further supported by the direct transmetalation of the **1**<sup>+</sup> with 1 equiv MeMgCl at –50 °C to generate the orange species **4**<sup>+</sup>, which upon warming to RT generates *p*-FPh-Me in 48% yield (Scheme 3).

The yield of *p*-FPh-Me during these oxidatively induced reductive elimination reactions (57 ± 4%) shows little dependence on the initial concentration of **1** (1–200 mM). Moreover, the oxidation of **4** with [Fc<sup>+</sup>]PF<sub>6</sub> in the presence of the radical trap TEMPO does not change the yield of *p*-FPh-Me (61 ± 1% yield) and <2% of the Me-TEMPO adduct is observed by GC-MS.<sup>54</sup> The EPR spectra of **4** in the presence of the spin trap DMPO, either in the absence or presence of FcPF<sub>6</sub>, reveal no radical adduct detectable by EPR, except for the radical impurity present in the DMPO (Figure S17). In addition, the reaction of [**1**<sup>+</sup>]PF<sub>6</sub> with MeMgCl in the presence of DMPO also does not generate any DMPO radical adduct.<sup>54</sup> Overall, these results suggest that the reactions occurring during the C–C reductive elimination of *p*-FPh-Me through the [(<sup>t</sup>BuN4)Ni<sup>III</sup>(PhF)Me]<sup>+</sup> intermediate most likely do not follow a radical mechanism.

Interestingly, **4**<sup>+</sup> exhibits a rhombic EPR spectrum with superhyperfine coupling to the two axial N atoms in the *z* direction, while the EPR spectrum of [(<sup>t</sup>BuN4)Ni<sup>III</sup>(PhF)(<sup>13</sup>CH<sub>3</sub>)]<sup>+</sup> (**13C-4**<sup>+</sup>), formed upon the treatment of **1**<sup>+</sup> with <sup>13</sup>CH<sub>3</sub>MgI, reveals broader signals in both the *x* and *z* directions due to additional superhyperfine coupling to the <sup>13</sup>C nuclei (*I* = 1/2) of the methyl group (Figure 4 and Table S7). The observed superhyperfine coupling to the <sup>13</sup>C nuclei of the equatorial Me ligand is likely due to the appreciable contribution of the Ni 3d<sub>*x*<sup>2</sup>–*y*<sup>2</sup></sub> orbital (22%) to the singly occupied molecular orbital (Figure 2B) and thus strongly suggests the presence of a Ni–Me bond. In addition, the DFT calculated EPR parameters and UV–vis spectrum of **4**<sup>+</sup> reproduce well the experimental results and further support

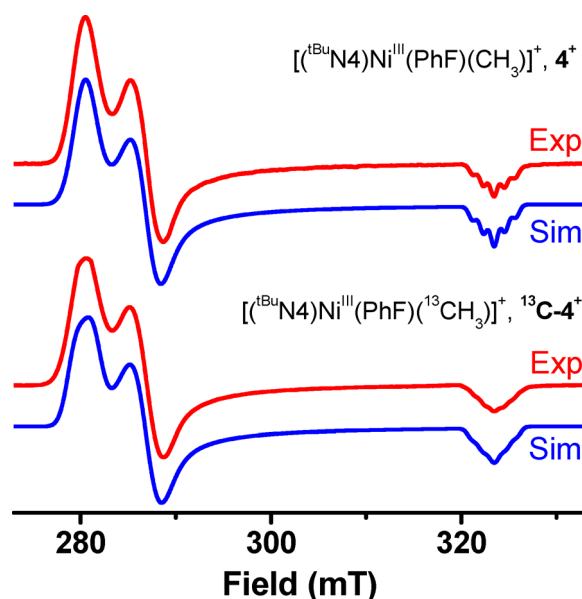
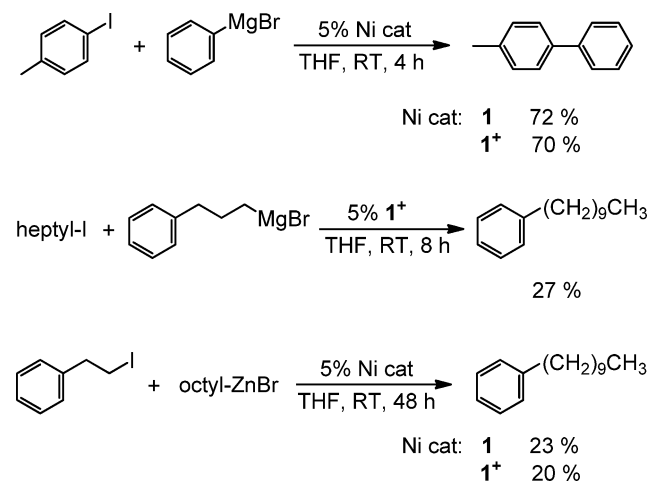


**Figure 4.** EPR spectra (red lines) of **4**<sup>+</sup> (top) and <sup>13</sup>C-**4**<sup>+</sup> (bottom) in 3:1:5 THF:Et<sub>2</sub>O:PrCN at 77 K, and the simulated EPR spectra (blue lines) using the following parameters: **4**<sup>+</sup>, *g*<sub>x</sub> = 2.317; *g*<sub>y</sub> = 2.265; *g*<sub>z</sub> = 2.009 (*A*<sub>N(2N)</sub> = 11.2 G); <sup>13</sup>C-**4**<sup>+</sup>, *g*<sub>x</sub> = 2.318 (*A*<sub><sup>13</sup>C</sub> = 17.0 G); *g*<sub>y</sub> = 2.265; *g*<sub>z</sub> = 2.009 (*A*<sub>N(2N)</sub> = 11.2 G, *A*<sub><sup>13</sup>C</sub> = 5.2 G), including superhyperfine coupling due to the <sup>13</sup>C–methyl group bonded to the Ni<sup>III</sup> center.

the formation of such a Ni<sup>III</sup> species.<sup>54</sup> A similar Ni<sup>III</sup>(aryl)alkyl species is generated upon the reaction of **1**<sup>+</sup> with octylzinc bromide, as observed by EPR (Figure S28). Overall, these studies suggest the formation of a detectable Ni<sup>III</sup>(aryl)alkyl intermediate that undergoes C–C reductive elimination, and therefore it is expected to be catalytically active in cross-coupling reactions (see below).

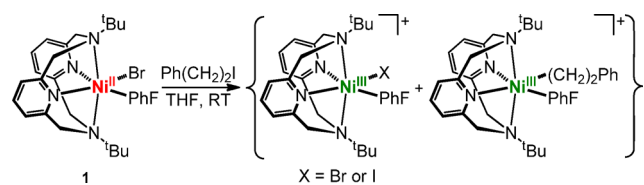
**Cross-Coupling Catalytic Reactivity of (<sup>t</sup>BuN4)Ni Complexes.** The organometallic Ni<sup>II</sup> and Ni<sup>III</sup> complexes described herein are active catalysts for Kumada and Negishi cross-coupling reactions (Scheme 4). For example, the coupling of iodotoluene with PhMgBr is accomplished in up to 72% unoptimized yield using either **1** or **1**<sup>+</sup> as the catalyst, while the

#### Scheme 4. Catalytic Activity of (<sup>t</sup>BuN4)Ni<sup>II</sup> and (<sup>t</sup>BuN4)Ni<sup>III</sup> Complexes in Kumada and Negishi Cross-Coupling Reactions



Kumada coupling of iodoheptane with an alkyl Grignard generates the product in 27% unoptimized yield using  $\mathbf{1}^+$  as the catalyst.<sup>54</sup> In addition, both  $\mathbf{1}$  and  $\mathbf{1}^+$  can catalyze the Negishi coupling of 1-octylzinc bromide with iodoethylbenzene in 23% and 20% unoptimized yields, respectively (Scheme 4), and a similar yield was obtained when iodopropylbenzene was used instead.<sup>54</sup> Interestingly, when  $\mathbf{1}$  is treated with 1 equiv iodoethylbenzene, the EPR spectrum of the resulting solution reveals the presence of two  $\text{Ni}^{\text{III}}$  signals that are tentatively assigned to a  $\text{Ni}^{\text{III}}(\text{aryl})\text{halide}$  and a  $\text{Ni}^{\text{III}}(\text{aryl})\text{alkyl}$  species, by comparison to the EPR spectra of analogous  $\text{Ni}^{\text{III}}$  complexes described above (Scheme 5 and Figure S29). This observation

**Scheme 5. Proposed Formation of Two  $\text{Ni}^{\text{III}}$  Species upon the Reaction of  $\mathbf{1}$  with Phenethyl Iodide**



is in line with the well-established radical scavenging ability of  $\text{Ni}^{\text{II}}$  complexes to generate  $\text{Ni}^{\text{III}}$  species in Kharasch radical additions, as reported by van Koten et al.<sup>65,66</sup> In addition, for both Kumada and Negishi cross-coupling reactions, formation of adducts between the organometallic reagent and the solvent (e.g., THF) was observed,<sup>54</sup> supporting radical mechanisms for both cross-coupling reactions, and also as observed recently by Fu et al.<sup>15</sup>

Since the seminal work of Kochi et al. more than three decades ago,<sup>8</sup> many experimental<sup>7-9,14-21,24,25,27,30,67</sup> and computational reports<sup>68-70</sup> have proposed the involvement of organometallic  $\text{Ni}^{\text{III}}$  intermediates in cross-coupling reactions. For example, Fu et al. proposed a radical mechanism for Ni-catalyzed cross-coupling reactions that involves  $\text{Ni}^{\text{I}}$  and  $\text{Ni}^{\text{III}}$  intermediates,<sup>15</sup> while Cardenas et al. have proposed the involvement of  $\text{Ni}^{\text{III}}(\text{Ar})\text{X}$  intermediates in transmetalation reactions of alkyl zinc reagents with aryl halides in Negishi cross-coupling.<sup>19,20</sup> Moreover, Vici et al. have proposed a  $\text{Ni}^{\text{III}}$ -dialkyl species as an intermediate in alkyl-alkyl Negishi coupling,<sup>16,17</sup> while Hu et al. have recently proposed a radical bimetallic oxidation mechanism for alkyl-alkyl Kumada coupling that involves two different  $\text{Ni}^{\text{III}}$  intermediates.<sup>67</sup> The involvement of alkyl radical species that generate a  $\text{Ni}^{\text{III}}(\text{aryl})\text{-alkyl}$  species has also been proposed in the cross-electrophile coupling of aryl halides with alkyl halides by Weix et al.<sup>27</sup> The reactivity studies of the organometallic  $(\text{tBuN4})\text{Ni}^{\text{III}}$  complexes reported herein provide strong evidence for these proposed reactions at  $\text{Ni}^{\text{III}}$  centers, such as the ability of an alkyl halide to oxidize a  $\text{Ni}^{\text{II}}\text{-aryl}$  species, most likely through a radical mechanism, as well as for the involvement of more than one  $\text{Ni}^{\text{III}}$  intermediate in these cross-coupling catalytic reactions.<sup>67</sup>

It is important to note that a large number of mechanisms have been proposed for the various Ni-catalyzed cross-coupling reactions,<sup>1-6</sup> and several of these mechanisms have suggested the involvement of  $\text{Ni}^{\text{III}}$  intermediates.<sup>7-31</sup> We have employed herein the described  $(\text{tBuN4})\text{Ni}^{\text{III}}$  complexes in stoichiometric transmetalation and reductive elimination reactions as well as Kumada and Negishi cross-coupling reactions that strongly supports their involvement in such catalytic transformations. This study does not attempt to provide an overall mechanism

for such reactions nor does it imply how such  $\text{Ni}^{\text{III}}$  can be generated under catalytic conditions (i.e., whether these species are formed by radical or nonradical mechanisms). However, we consider these studies open up the possibility of detailed mechanistic studies of various cross-coupling reactions, which are the focus of our current research efforts.

## CONCLUSION

The studies reported herein provide for the first time strong evidence that organometallic  $\text{Ni}^{\text{III}}$  species are catalytically relevant in Ni-catalyzed cross-coupling reactions, which have been proposed to involve such  $\text{Ni}^{\text{III}}$  intermediates for more than three decades. The use of the tetradentate  $\text{tBuN4}$  ligand allowed the isolation and characterization of several  $\text{Ni}^{\text{III}}(\text{aryl})$  and  $\text{Ni}^{\text{III}}(\text{aryl})\text{alkyl}$  complexes and thus provided a unique opportunity to investigate their reactivity in oxidation, transmetalation, and reductive elimination steps that are essential for the catalytic cross-coupling reactions. A detailed understanding of the reactivity of organometallic odd-electron Ni complexes requires a range of spectroscopic and mechanistic studies that are essential for the development of more efficient and selective catalysts for various C–C and C–heteroatom organic transformations.

## ASSOCIATED CONTENT

### Supporting Information

Synthetic details, spectroscopic characterization, stoichiometric and catalytic reactivity studies, computational details, and crystallographic data. This material is available free of charge via the Internet at <http://pubs.acs.org>.

## AUTHOR INFORMATION

### Corresponding Author

mirica@wustl.edu

### Notes

The authors declare no competing financial interest.

## ACKNOWLEDGMENTS

We thank the American Chemical Society Petroleum Research Fund (52988-ND3) and the National Science Foundation (CHE-1255424) for support. L.M.M. is also supported by a Sloan Research Fellowship.

## REFERENCES

- (1) *Metal-Catalyzed Cross-Coupling Reactions*; Meijere, A. d., Diederich, F., Eds.; Wiley-VCH: Weinheim, Germany, 2004.
- (2) Netherton, M. R.; Fu, G. C. *Adv. Synth. Catal.* **2004**, *346*, 1525.
- (3) Frisch, A. C.; Beller, M. *Angew. Chem., Int. Ed.* **2005**, *44*, 674.
- (4) Phapale, V. B.; Cardenas, D. J. *Chem. Soc. Rev.* **2009**, *38*, 1598.
- (5) Rudolph, A.; Lautens, M. *Angew. Chem., Int. Ed.* **2009**, *48*, 2656.
- (6) Knochel, P.; Thaler, T.; Diene, C. *Isr. J. Chem.* **2012**, *50*, 547.
- (7) Tsou, T. T.; Kochi, J. K. *J. Am. Chem. Soc.* **1978**, *100*, 1634.
- (8) Tsou, T. T.; Kochi, J. K. *J. Am. Chem. Soc.* **1979**, *101*, 7547.
- (9) Amatore, C.; Jutand, A. *Organometallics* **1988**, *7*, 2203.
- (10) Zhou, J.; Fu, G. C. *J. Am. Chem. Soc.* **2004**, *126*, 1340.
- (11) Powell, D. A.; Fu, G. C. *J. Am. Chem. Soc.* **2004**, *126*, 7788.
- (12) Owston, N. A.; Fu, G. C. *J. Am. Chem. Soc.* **2010**, *132*, 11908.
- (13) Zultanski, S. L.; Fu, G. C. *J. Am. Chem. Soc.* **2011**, *133*, 15362.
- (14) Dudnik, A. S.; Fu, G. C. *J. Am. Chem. Soc.* **2012**, *134*, 10693.
- (15) Zultanski, S. L.; Fu, G. C. *J. Am. Chem. Soc.* **2013**, *135*, 624.
- (16) Jones, G. D.; McFarland, C.; Anderson, T. J.; Vici, D. A. *Chem. Commun.* **2005**, 4211.

- (17) Jones, G. D.; Martin, J. L.; McFarland, C.; Allen, O. R.; Hall, R. E.; Haley, A. D.; Brandon, R. J.; Konovalova, T.; Desrochers, P. J.; Pulay, P.; Vivic, D. A. *J. Am. Chem. Soc.* **2006**, *128*, 13175.
- (18) Klein, A.; Budnikova, Y. H.; Sinyashin, O. G. *J. Organomet. Chem.* **2007**, *692*, 3156.
- (19) Phapale, V. B.; Bunuel, E.; Garcia-Iglesias, M.; Cardenas, D. J. *Angew. Chem., Int. Ed.* **2007**, *46*, 8790.
- (20) Phapale, V. B.; Guisan-Ceinós, M.; Bunuel, E.; Cardenas, D. J. *Chem.—Eur. J.* **2009**, *15*, 12681.
- (21) Gong, H. G.; Gagné, M. R. *J. Am. Chem. Soc.* **2008**, *130*, 12177.
- (22) Gong, H. G.; Andrews, R. S.; Zuccarello, J. L.; Lee, S. J.; Gagné, M. R. *Org. Lett.* **2009**, *11*, 879.
- (23) Vechorkin, O.; Hu, X. *Angew. Chem., Int. Ed.* **2009**, *48*, 2937.
- (24) Vechorkin, O.; Proust, V. r.; Hu, X. *J. Am. Chem. Soc.* **2009**, *131*, 9756.
- (25) Hu, X. *Chem. Sci.* **2011**, *2*, 1867.
- (26) Everson, D. A.; Shrestha, R.; Weix, D. J. *J. Am. Chem. Soc.* **2010**, *132*, 920.
- (27) Biswas, S.; Weix, D. J. *J. Am. Chem. Soc.* **2013**, *135*, 16192.
- (28) Joshi-Pangu, A.; Wang, C. Y.; Biscoe, M. R. *J. Am. Chem. Soc.* **2011**, *133*, 8478.
- (29) Yu, X. L.; Yang, T.; Wang, S. L.; Xu, H. L.; Gong, H. G. *Org. Lett.* **2011**, *13*, 2138.
- (30) Dai, Y. J.; Wu, F.; Zang, Z. H.; You, H. Z.; Gong, H. G. *Chem.—Eur. J.* **2012**, *18*, 808.
- (31) Xu, H.; Zhao, C.; Qian, Q.; Deng, W.; Gong, H. *Chem. Sci.* **2013**, *4*, 4022.
- (32) Matsunaga, P. T.; Hillhouse, G. L.; Rheingold, A. L. *J. Am. Chem. Soc.* **1993**, *115*, 2075.
- (33) Koo, K.; Hillhouse, G. L. *Organometallics* **1995**, *14*, 4421.
- (34) Koo, K. M.; Hillhouse, G. L.; Rheingold, A. L. *Organometallics* **1995**, *14*, 456.
- (35) Han, R. Y.; Hillhouse, G. L. *J. Am. Chem. Soc.* **1997**, *119*, 8135.
- (36) Lin, B. L.; Clough, C. R.; Hillhouse, G. L. *J. Am. Chem. Soc.* **2002**, *124*, 2890.
- (37) Ragsdale, S. W. *J. Biol. Chem.* **2009**, *284*, 18571.
- (38) Ermler, U.; Grabarse, W.; Shima, S.; Goubeaud, M.; Thauer, R. *K. Science* **1997**, *278*, 1457.
- (39) Riordan, C. G. *J. Biol. Inorg. Chem.* **2004**, *9*, 542.
- (40) Evans, D. J. *Coord. Chem. Rev.* **2005**, *249*, 1582.
- (41) Yang, N.; Reiher, M.; Wang, M.; Harmer, J.; Duin, E. C. *J. Am. Chem. Soc.* **2007**, *129*, 11028.
- (42) Dey, M.; Telsler, J.; Kunz, R. C.; Lees, N. S.; Ragsdale, S. W.; Hoffman, B. M. *J. Am. Chem. Soc.* **2007**, *129*, 11030.
- (43) Lee, C. M.; Chen, C. H.; Liao, F. X.; Hu, C. H.; Lee, G. H. *J. Am. Chem. Soc.* **2010**, *132*, 9256.
- (44) Lipschutz, M. I.; Yang, X.; Chatterjee, R.; Tilley, T. D. *J. Am. Chem. Soc.* **2013**, *135*, 15298.
- (45) Scheller, S.; Goenrich, M.; Boecher, R.; Thauer, R. K.; Jaun, B. *Nature* **2010**, *465*, 606.
- (46) Scheller, S.; Goenrich, M.; Mayr, S.; Thauer, R. K.; Jaun, B. *Angew. Chem., Int. Ed.* **2010**, *49*, 8112.
- (47) Khusnutdinova, J. R.; Rath, N. P.; Mirica, L. M. *J. Am. Chem. Soc.* **2010**, *132*, 7303.
- (48) Khusnutdinova, J. R.; Rath, N. P.; Mirica, L. M. *J. Am. Chem. Soc.* **2012**, *134*, 2414.
- (49) Tang, F.; Qu, F.; Khusnutdinova, J. R.; Rath, N. P.; Mirica, L. M. *Dalton Trans.* **2012**, *41*, 14046.
- (50) Mirica, L. M.; Khusnutdinova, J. R. *Coord. Chem. Rev.* **2013**, *299*.
- (51) Marshall, W. J.; Grushin, V. V. *Can. J. Chem.* **2005**, *83*, 640.
- (52) Meneghetti, S. P.; Lutz, P. J.; Fischer, J.; Kress, J. *Polyhedron* **2001**, *20*, 2705.
- (53) Khusnutdinova, J. R.; Luo, J.; Rath, N. P.; Mirica, L. M. *Inorg. Chem.* **2013**, *52*, 3920.
- (54) See Supporting Information.
- (55) Grove, D. M.; van Koten, G.; Mul, W. P.; Vanderzeijden, A. A. H.; Terheijden, J.; Zoutberg, M. C.; Stam, C. H. *Organometallics* **1986**, *5*, 322.
- (56) van de Kuil, L. A.; Veldhuizen, Y. S. J.; Grove, D. M.; Zwikker, J. W.; Jenneskens, L. W.; Drenth, W.; Smeets, W. J. J.; Spek, A. L.; van Koten, G. *J. Organomet. Chem.* **1995**, *488*, 191.
- (57) Grove, D. M.; van Koten, G.; Zoet, R.; Murrall, N. W.; Welch, A. J. *J. Am. Chem. Soc.* **1983**, *105*, 1379.
- (58) Grove, D. M.; van Koten, G.; Mul, P.; Zoet, R.; van der Linden, J. G. M.; Legters, J.; Schmitz, J. E. J.; Murrall, N. W.; Welch, A. J. *Inorg. Chem.* **1988**, *27*, 2466.
- (59) Iluc, V. M.; Miller, A. J. M.; Anderson, J. S.; Monreal, M. J.; Mehn, M. P.; Hillhouse, G. L. *J. Am. Chem. Soc.* **2011**, *133*, 13055.
- (60) Ceder, R. M.; Granell, J.; Muller, G.; FontBardia, M.; Solans, X. *Organometallics* **1996**, *15*, 4618.
- (61) Higgs, A. T.; Zinn, P. J.; Simmons, S. J.; Sanford, M. S. *Organometallics* **2009**, *28*, 6142.
- (62) Higgs, A. T.; Zinn, P. J.; Sanford, M. S. *Organometallics* **2010**, *29*, 5446.
- (63) Han, R.; Hillhouse, G. L. *J. Am. Chem. Soc.* **1998**, *120*, 7657.
- (64) Zhang, C. P.; Wang, H.; Klein, A.; Biewer, C.; Stimat, K.; Yarnaguchi, Y.; Xu, L.; Gomez-Benitez, V.; Vivic, D. A. *J. Am. Chem. Soc.* **2013**, *135*, 8141.
- (65) Gossage, R. A.; van de Kuil, L. A.; van Koten, G. *Acc. Chem. Res.* **1998**, *31*, 423.
- (66) Kleij, A. W.; Gossage, R. A.; Klein Gebbink, R. J. M.; Brinkmann, N.; Reijerse, E. J.; Kragl, U.; Lutz, M.; Spek, A. L.; van Koten, G. *J. Am. Chem. Soc.* **2000**, *122*, 12112.
- (67) Breitenfeld, J.; Ruiz, J.; Wodrich, M. D.; Hu, X. *J. Am. Chem. Soc.* **2013**, *135*, 12004.
- (68) Lin, X. F.; Phillips, D. L. *J. Org. Chem.* **2008**, *73*, 3680.
- (69) Li, Z.; Jiang, Y. Y.; Fu, Y. *Chem.—Eur. J.* **2012**, *18*, 4345.
- (70) Lin, X. F.; Sun, J.; Xi, Y. Y.; Lin, D. L. *Organometallics* **2011**, *30*, 3284.